ARTICLES

A Phenomenological Model of Volumetric and Free Volume Hole Properties in Supercooled Liquids: The *ortho*-Terphenyl Case

J. Bartoš[†,]* and J. Krištiak[‡]

Polymer Institute of SAS, Dúbravská cesta 9, SK-842 36 Bratislava, Slovak Republic, and Institute of Physics of SAS, Dúbravská cesta 9, SK 842 28 Bratislava

Received: October 27, 1999; In Final Form: February 18, 2000

A phenomenological model linking the macroscopic volume from dilatometry with the microscopic free volume from positron annihilation lifetime spectroscopy is presented. The temperature dependences of both quantities enable to obtain the so-called initial temperature T_i at which dynamic free volume change sets in, the corresponding initial volume V_i, and subsequently, all free volume characteristics. Application of this model on the literature data of a typical low-molecular weight glass former, *o*-terphenyl, leads to the findings that (i) $T_i \cong T_K$ the Kauzmann temperature and (ii) a packing fraction of the extrapolated equilibrium liquid at T_i is close to the closest regular packing of hard spheres. The published viscosity−temperature data over 12 decades of magnitude are correlated with the free volume hole fraction f_h, as determined from the PALS results, via the WLF−Doolittle type equation. These findings indicate that the orthopositronium (*o*-Ps) is able to detect the part of the total free volume distribution which is relevant for the viscosity over the measured temperature interval from T_g up to $\sim 1.5T_g$. In addition, the change of the free volume hole behavior above $T_r = 1.25T_g$, lying in the vicinity of the crossover temperature T_c from the idealized version of mode-coupling theory, is critically analyzed within a modified bubble concept (the equilibrium interaction of o-Ps with the soft matrix).

I. Introduction

The physical nature of the dynamics of supercooled liquids as well as of the liquid−glass transition is still a very actual challenge of the condensed matter physics.[1a−f] A wide spectrum of disordered materials ranging from inorganic (including metals) compounds to organic, both low- and high-molecular weight ones, exhibits this phenomenon. Despite their huge chemical diversity, thermodynamic and dynamic phenomenologies of the supercooled liquids have remarkably universal features: (i) thermodynamic properties such as volume and enthalpy give a bend at the conventionally defined glass transition temperature T_g. and (ii) transport (mobility) properties M, such as viscosity ($M = \eta$), relaxation time ($M = \tau$), and diffusion coefficient ($M = 1/D$) exhibit the deviations from the "ideal" Arrhenius and Debye laws for temperature or time dependences, respectively.

A number of models and theories have been formulated to explain these findings which are based on a variety concepts such as free volume,[1c] excess entropy,[1a] or purely dynamic change due to mode coupling.[1d] To follow our approach, we review briefly the relevant phenomenology and some of the related treatments, especially those based on the free volume idea.

Volumetric and Free Volume Hole Properties. Dilatometry belongs to the classical methods to investigate a variety aspects of the liquid−glass transition.[2] The most important phenomenon of any amorphous phase is characterized by an abrupt change in the slope on the $V-T$ diagram, i.e., by a jump change in the macroscopic volume expansivity $\beta_V = \Delta V/\Delta T$ or in the macroscopic volume expansion coefficient $\alpha_V = (1/V_g)(\Delta V/\Delta T)$, see Figure 1.

On the other hand, positron annihilation lifetime spectroscopy (PALS) becomes a very powerful tool for extensive study of the free volume microstructure in disordered materials during the past decade.[3,4] The orthopositronium (o-Ps) is a very sensitive microscopic probe to detect the defective regions such as holes, vacancies, cavities.[5]

A semiempirical quantum-mechanical model has been formulated which relates the orthopositronium lifetime τ_3 to the effective free volume hole radius R_h as follows:

$$\tau_3 = {}^1/_2[1 - (R_h/R_0) + ({}^1/_2\pi)\sin(2\pi R_h/R_0)]^{-1} \qquad (1)$$

where $R_0 = R_h + \Delta R$, $\Delta R = 1.66$ Å, is a fitting parameter from the observed o-Ps lifetimes for several groups of materials with the known hole radii such as zeolites and molecular crystals.

In the glass-liquid transition region, the free volume holes R_h (or V_h) behave in a similar way as the macroscopic volume exhibiting the rapid slope change at around T_g. An essential difference in the corresponding temperature expansion coefficients exists. While the macroscopic volume expansion coefficients α_V are of the order of magnitude of 10^{-4} K^{-1} for both

* Corresponding author. E-mail: upolbrts@savba.sk.
† Polymer Institute of SAS.
‡ Institute of Physics of SAS.

10.1021/jp993703f CCC: $19.00
Published on Web 05/27/2000

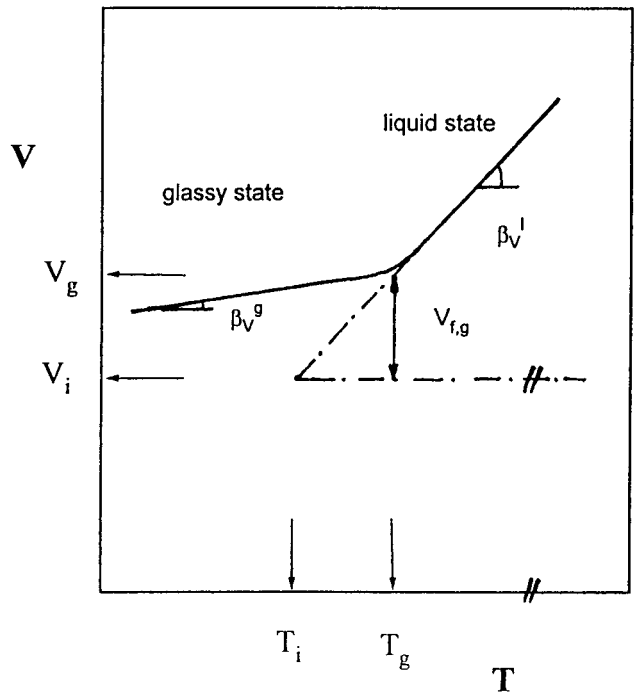

Figure 1. Schematic plot of the volumetric and free volume properties in the glass−liquid transition region of amorphous material.

glassy and viscous liquid state,[2] the free volume hole expansion coefficients $\alpha_{Vh} = (1/V_{h,g})(\Delta V_h/\Delta T)$ are 1 or even 2 orders of magnitude higher below or above T_g, respectively.[3,7−9] The second o-Ps annihilation quantity from PALS method, the relative o-Ps intensity I_3, is believed to be related to the number of free volume holes and consequently, a semiempirical relationship between the free volume hole fraction $f_h(T)$ and both the annihilation characteristics has been presented:

$$f_h(T) = K_{Vh} V_h(T) I_3(T) \tag{2}$$

[10,11] where V_h is the mean free volume hole size obtained from eq 1 as $V_h = (4\pi/3)R_h^3$ and K_{Vh} is a proportionality coefficient. This coefficient can be determined by various calibration procedures using other physical quantities such as the difference of the volume expansion coefficients below and above T_g[11,12] or by the present phenomenological approach.

Dynamic Properties. Phenomenologically, the dynamic behavior of supercooled liquids can be described in two different ways depending on the chosen independent variable. The first group of approaches is represented by various empirical formulas, such as the Vogel−Fulcher−Tammann−Hesse (VFTH) equation[13] or, equivalently, by the Williams−Landel−Ferry (WLF) one,[14] for both relatively low and high-temperature ranges with respect to T_g:[15]

$$\text{VFTH:} \qquad M(T) = A_T \exp[B_T/(T - T_0)] \tag{3}$$

or

$$\text{WLF:} \quad a(T) = M(T)/M(T_g) = \exp[-C_{1g}(T - T_g)/(C_{2g} + T - T_g)] \tag{4}$$

The other description of the liquid mobilities is based on the free volume concept[16] and is represented by the semiempirical Doolittle equation:[17]

$$M(T) = A_f \exp[B_f/f(T)] \tag{5}$$

where $f(T)$ is the free volume fraction defined as $f(T) = V_f(T)/V(T)$, V_f being appropriately defined free volume, and $V(T)$ is the macroscopic volume from dilatometric measurements. Formally, eqs 3 and 5 are equivalent, assuming:

$$f(T) = \beta_f^l (T - T_0) \tag{6}$$

where β_f^l is the slope of f vs T dependence in the liquid state and T_0 is the Vogel temperature at which the corresponding mobility disappears due to $f \rightarrow 0$. In the above-mentioned eqs 3−5, all the quantities besides the liquid mobilities are parameters physical meaning of which needs to be established via various theoretical treatments or/and independent experiments.

One group of theoretical treatments[16−20] tries to connect the dynamics with thermodynamics based on the free volume[16−19] or excess entropy[20] concept. The original free volume interpretation of the transport properties[18] is based on a combination of the statistical−mechanical model of transport properties resulting into an exponential form for the mobility under assumption of linear temperature dependence of free volume. An extended version of the free volume model[19] using percolation ideas leads to more complicated multiparameter form for $f(T)$ dependence.

Application of the Doolittle eq 5 becomes very useful in interpretation of the WLF eq 4, especially in polymer physics.[1c,14] Under the assumption that

$$f(T) = f(T_g) + \beta_f^l (T - T_0) \tag{7}$$

one can arrive to the following free volume expressions for the C_{1g} and C_{2g} parameters:

$$C_{1g} = B_f/f_g \quad C_{2g} = f_g/\beta_f^l \tag{8a,b}$$

And further, under the assumption that $B_f = 1$, one can *estimate* the free volume fraction at T_g, $f(T_g) \equiv f_g$, and the expansivity of the free volume fraction β_f^l; the former being about 2−3%, the latter $\beta_f^l \cong \Delta\alpha_V = \alpha_V^l - \alpha_V^g \sim 10^{-4}$ K^{-1}, where α_V^l, α_V^g are the macroscopic volume expansion coefficients above and below T_g[14]. Strictly speaking, the estimation of these free volume characteristics relies on both the mentioned assumptions and they are the results of the corresponding fits. Thus, their verification or determination of the f values by means of independent procedure is needed.

As for the Adam−Gibbs entropy model of dynamic behavior of supercooled liquids,[20a] the excess configurational entropy of a liquid over that of the corresponding crystal from calorimetric studies is assumed to vanish at a temperature T_2 identified by Gibbs and DiMarzio as a second-order transition temperature.[20b] So T_2 is closely related to the Kauzmann temperature T_K, at which an extrapolated liquid entropy reaches that of the crystal phase.[21−23] It is noteworthy that in many cases the Vogel divergence temperature T_0 lies in the vicinity of the Kauzmann temperature as reported by several authors.[19b,22,23] The existence of the so-called ideal glass associated with an underlying phase transition below the measured glass transition temperature T_g is discussed topic until now.[24]

From the above-mentioned review, direct verification of some basic assumptions of the free volume theory and of the related empirical equations is very actual. This paper presents a phenomenological model linking the macroscopic volumetric behavior of supercooled liquid to the microscopic free volume hole properties in order to quantify the free volume hole fraction, section II. This model is applied on a typical low-molecular

weight glass former of a van der Waals type: *o*-terphenyl (OTP), section III. OTP has been selected because it belongs to the widest studied and probably to the best understood fragile materials from the dynamic point of view. The wealth of the thermodynamic, o-Ps annihilation, and various dynamic data enables us not only to apply our approach but also to discuss its outputs from both microscopic, as well as macroscopic, dynamic viewpoints. Direct empirical relationship between the free volume hole data and typical transport quantity has been established. Finally, we discuss the model outputs from the points of view of the free volume and entropy models of dynamics in supercooled liquids, section IV.

II. Phenomenological Model

The macroscopic specific volume, $V(T)$, at a temperature T from the temperature range of the liquid state, $T > T_g$, can be represented in the simplest approximation in a linear form as follows:

$$V(T) = V_i[1 + \alpha_V^l(T - T_i)] \tag{9}$$

where α_V^l is the macroscopic volume expansion coefficient and V_i and T_i are the free parameters of our model which have to be determined and their physical meanings established. Thus, the free volume $V_f(T)$ is the excess volume over some reference state V_i is given by

$$V_f(T) = V(T) - V_i = \alpha_V^l V_i(T - T_i) \tag{10}$$

where T_i is the so-called initial temperature at which the free volume begins to appear, Figure 1. The free volume fraction $f(T)$ at the temperature T is defined as

$$f(T) = V_f(T)/V(T) \tag{11}$$

and after substitution of eq 10 we have

$$f(T) = \alpha_V^l(T - T_i)/[1 + \alpha_V^l(T - T_i)] \tag{12}$$

The expansion coefficient of the free volume fraction is defined as

$$\alpha_f = [1/f(T_1)]\{[f(T_2) - f(T_1)]/(T_2 - T_1)\} \tag{13}$$

After substitution of eq 12 and simple algebraic manipulations for $T_1 = T_g$ and $T_2 = T$, we obtain an expression,

$$\alpha_f^l = [1/(T - T_g)]\{\{[(T - T_i)/(T_g - T_i)]\{[1 + \alpha_V^l(T_g - T_i)]/[1 + \alpha_V^l(T - T_i)]\} - 1\}\} \tag{14}$$

After several simple algebraic operations, we arrive to the final quadratic equation with respect to T_i:

$$T_i^2 + bT_i + c = 0 \tag{15}$$

where the coefficients read as

$$b = -[1 + \alpha_V^l(T_g + T)]/\alpha_V \tag{16a}$$

$$c = [(1 + \alpha_V^l T)T_g]/\alpha_V^l + [(1 + \alpha_V^l T)T_g]/[\alpha_f^l(T - T_g)\alpha_V^l] - [(1 + \alpha_V^l T_g)T]/[\alpha_f^l(T - T_g)\,\alpha_V^l] \tag{16}$$

In the context of the PALS measurements, the free volume fraction $f(T)$ may be identified with the free volume hole fraction $f_h(T)$, given by eq 2 in section I. Then, the expansion coefficient of the free volume hole fraction $\alpha_{f,h}^l$ can easily be obtained from the measured τ_3 and I_3 data using eqs 1 and 2:

$$\alpha_{fh}^l = [1/(V_h I_3)_g][\Delta(V_h I_3)/\Delta T] \tag{17}$$

Consequently, the quadratic eq 15can be solved with respect to T_i.

III. Application on OTP

Dilatometric investigations on OTP were performed by several research groups.[25−27]

The most extended and detailed data are given by Naoki and Koeda.[27] Their $p-V-T$ results on OTP covering very wide temperature range from 220 up to 415 K, including both glassy and liquid phases, as well as the crystalline, are expressed in a polynomial form in T and p:

$$V(T,p) = \sum_{i=0}\sum_{j=0} c(i,j)T^i p^j \tag{18}$$

where $c(i,j)$ are the empirical parameters depending on the phase state considered.[27]

The linearity of V on T required by eq 9 is satisfactorily fulfilled in a temperature region of our interest from 250 up to 290 K. Thus, one can obtain the mean expansion coefficient $\alpha_V^l = 7.31 \times 10^{-4}$ K^{-1}.

The detailed PALS study on OTP in both glassy and liquid states from 220 up to 365 K was performed by Malhotra and Pethrick.[28,29] The temperature dependences of both the relevant o-Ps annihilation quantities τ_3 and I_3 are presented in Figure 1 of ref 28. τ_3-T plot for amorphous OTP exhibits three regions of different behavior:

(i) glassy region from 220K up to about 240K in accord with the glass transition temperature $T_g = 243$K,[25] (ii) low-temperature liquid region from 245 up to around $T_r \cong 304$ K, and finally (iii) high-temperature liquid region above T_r continuing beyond the melting temperature of the crystalline form of OTP, $T_m = 331$ K.[25] Therefore, we shall analyze these qualitatively different regions of liquid state separately.

Low-Temperature Viscous Liquid Region. In the context of our model just formulated in section II, we analyze the low-temperature region of viscous liquid (ii). The following higher temperature region of fluid liquid state iii will be discussed afterward.

The mean o-Ps lifetime τ_3, the mean free volume hole radius R_h, calculated using eq 1 (Figure 2) and, consequently, the mean hole volumes $V_h = (4\pi/3)R_h^3$ can be represented by the following empirical equations:

$$\tau_3[\text{ns}] = 1.59 \times 10^{-2}T - 2.34 \qquad r = 0.994 \tag{19a}$$

$$R_h[\text{Å}] = 1.48 \times 10^{-2}T - 1.21 \qquad r = 0.996 \tag{19b}$$

$$V_h[\text{Å}^3] = 1.48T - 307.38 \qquad r = 0.989 \tag{19c}$$

where r is the regression coefficient. The corresponding free volume hole expansion coefficient α_{Vh}^l can be obtain from the slope of eq 19c and the value of free volume hole size at T_g, $V_{hg} = V_h(T_g) = 56$ Å^3, i.e., 2.56×10^{-2} K^{-1}. This value is almost 2 orders of magnitude larger than that of the macroscopic volume $\alpha_V^l = 7.31 \times 10^{-4}$ K^{-1} in accord with the previous experiences.[3,7−9] The second annihilation characteristic, the o-Ps relative intensity I_3, is a measure of o-Ps formation probability and, thus, of the number of free volume holes detectable by this microscopic probe.[3−7,10−12] Figure 1 of ref 28 shows that

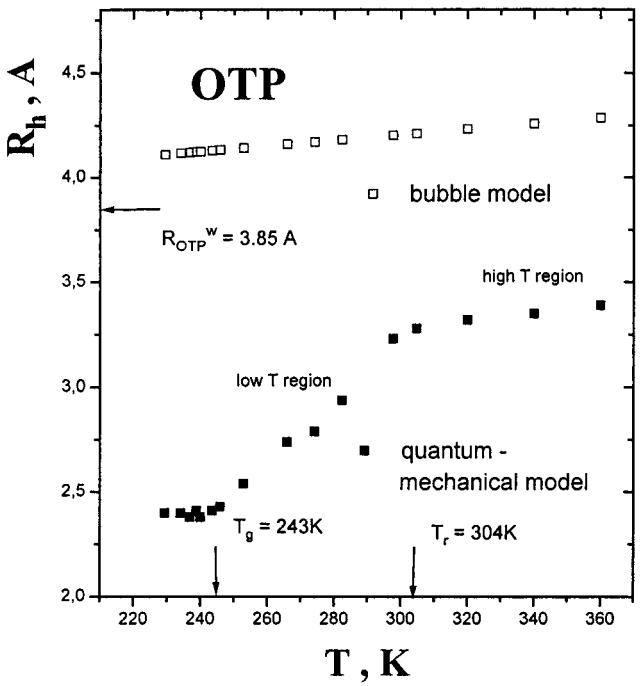

Figure 2. The temperature dependence of the free volume hole radius R_h as determined from the PALS data (ref 28) by means of a quantum-mechanical model, eq 1, and of the bubble radius r_b as calculated by using eq 24.

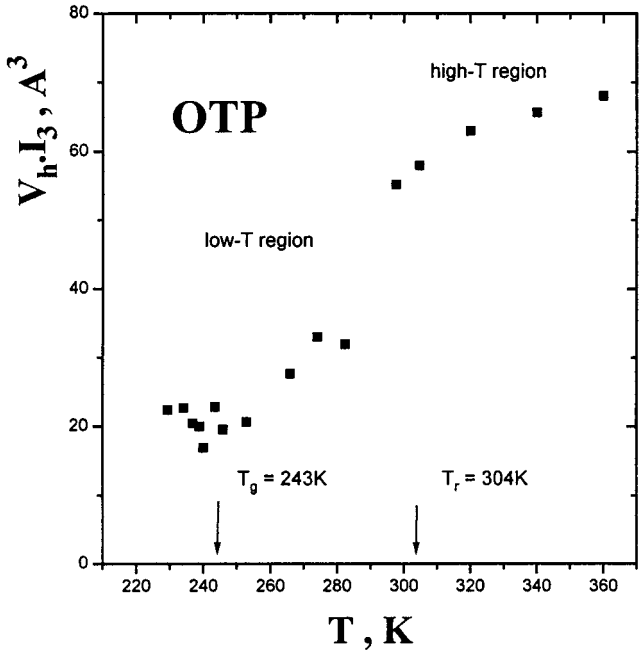

Figure 3. The temperature dependence of the product of the hole volumeV_h and the o-Ps relative intensity I_3 from ref 28.

the change of I_3 with the temperature is rather weak over a wide temperature range from below T_g through the viscous liquid regime up to the fluid liquid region well above T_m. Figure 3 gives the temperature dependence of the product of $V_h(T)I_3(T)$. A least-squares regression analysis provides the expansion coefficient of the free volume hole fraction $\alpha_{fh}^{l} = 2.8 \times 10^{-2}$ K^{-1} with the regression coefficient 0.988. Then, eq 15 can be solved with respect to T_i. The results are calculated to be $T_{i,1} =$ 209 K and $T_{i.2} =$ 1693 K. We note that the solution is very stable because it is not very sensitive to the changes of α_V^{l}, α_{fh}^{l} as well as to choice of the upper boundary temperature T. This indicates the robustness of solution of eq 15.

High-Temperature Fluid Liquid Region. In this section we analyze the high-temperature liquid region above $T_r = 304$ K.

The relevant quantities can be approximated by the following equations:

$$\tau_3[\text{ns}] = 2.40 \times 10^{-3}T + 1.78 \qquad r = 0.998 \quad (20a)$$

$$R_h[\text{Å}] = 1.82 \times 10^{-3}T + 2.73 \qquad r = 0.996 \quad (20b)$$

The relatively large change of the temperature dependences of τ_3 and R_h at around T_r seems to indicate some change of the mechanism of a mutual interaction between the o-Ps probe and the low viscosity fluid liquid. The same finding, i.e., slight increase of τ_3 and I_3 with T at relative higher temperatures with respect to T_g have also been found by us in a typical polymer: *cis*-1,4-polybutadiene.[9] In the original work on OTP,[28] this effect was attributed to the so-called bubble state of o-Ps in relatively soft liquid matrix.[30,31] This proposal was based on the data fitting by using a semiempirical relation between τ_3 and macroscopic surface tension γ_∞: $1/\tau_3 = a\gamma^b$, where the coefficient a and the exponential b reach the typical values for the simple liquids of low viscosity.

But this Tao's relationship uses the surface tension only instead of complete consideration of both the surface tension and internal pressure term.[33,9] Assuming that the energy of o-Ps in a medium is at the minimum, then the expression 21 follows from the balance between outward pressure due to quantum zero-point motion of o-Ps and inward pressure due to surface tension γ_∞ and internal pressure p_{int}:[32,9]

$$(\pi h)^2/4m_e r_b^{\,2} = 4\pi r_b^{\,2}\gamma_\infty + (4\pi/3)r_b^{\,3}p_{int} \qquad (21)$$

where m_e is the mass of positron and r_b is the bubble radius. To test this hypothesis we have calculated as the first approximation the temperature dependence of the bubble radius over the whole temperature liquid range from 250 up to 360 K using the γ_∞ data from original paper.[28] The internal pressure was calculated from the $V-T$ data of dilatometric work[27] using the reported empirical equation for the thermal pressure coefficient and the standard thermodynamic relation: $p_{int} = T\gamma_{th} - p_{ext}$, where p_{ext} is the external pressure. The results of calculation of the bubble radius can be described by

$$r_b\,[\text{Å}] = 1.4 \times 10^{-3}T + 3.6 \qquad (22)$$

over the entire temperature interval of the liquid state. We note that the second term in eq 21 is of essential importance because of its proportion of 54% at 250 K and of 62% at 360 K. Thus, the modified bubble concept given by eq 21 seems to be more reliable then an application of Tao's relation only. Despite this progress, eq 21 can suffers from the use of macroscopic surface tension because the curvature of surface is believed to play some role.[34] Byakov et al.[35] have very recently solved this problem by simultaneous measurements of the o-Ps lifetime and of the angular correlation of annihilation gamma photons. For a wide series of 28 liquids of simple, complex and chain structure they found that the microscopic surface tension γ (r) can be accounted for by the Tolman equation:[36]

$$\gamma\,(r) = \gamma_\infty/[1 + (2\delta/r)] \qquad (23)$$

where δ is the thickness of surface layer around the spherical bubble. This parameter was generally found to be $0 < 2\delta < R_{cage}$; the first limit case $\delta = 0$ holds for symmetric and longer chain molecules in agreement with our recent result on *cis*-1,4-

polybutadiene[9] and the other limit is valid for asymmetric molecules. Since OTP molecules have a rather asymmetric shape we have applied the modified form of eq 21 with $\gamma(r)$ from eq 23 and $2\delta = R_{cage}(T)$. The last quantity was taken to be equal to the equivalent radius $R_{eq}^{mol}(T)$ calculated from the molar volume using $V-T$ data from ref 27. The results of calculations can be expressed by a linear equation,Comparison with eq 22

$$r_b[\text{Å}] = 1.35 \times 10^{-3}T + 3.8 \qquad (24)$$

shows rather small change of the coefficients and suggests a relative insensitivity to the correction on the curvature of surface. We note that the proportion of the volume work, i.e., the second term in eq 21 is enhanced from 71.5% at 250 K up to 77.5% at 360 K. The calculated temperature dependence of the bubble radius from eq 24 is plotted in Figure 2.

IV. Discussion

Glass-Liquid Transition and Viscous Liquid Region. The T_i values obtained from eq 15 can be discussed as follows. Evidently, $T_{i,2} = 1693$ K has no physical meaning because it is far above the usual decomposition temperature of ordinary organic compounds. On the other hand, $T_{i,1} = 209$ K lies below T_g. To determine its physical nature, we compare this initial temperature of free volume change with several characteristic temperatures of OTP which are situated below the thermodynamic glass transition temperature T_g. These quantities have been determined by a large number of the authors using various thermodynamic and dynamic methods, and they are summarized in Table 1.

The $T_{i,1}$ value is comparable with the Kauzmann temperature $T_K = 200 \pm 10$ K[22,37-39] at which the extrapolated liquid entropy reaches that of the corresponding crystalline form.[21-23] This fact suggests that infinitely slow cooling of the liquid could lead to some limiting state characterized by V_i. Knowing the macroscopic specific volume of supercooled liquid $V(T)$ and having $T_{i,1}$ as a solution of eq 15, we can calculated this hypothetical initial volume from eq 9. The result is $V_i = 0.8684$ cm^3 g^{-1}. Subsequently, the packing fraction p_i at $T_{i,1}$, defined as the ratio of the occupied (van der Waals) volume from an additive group scheme[42] ($V^w = 0.6268$ cm^3 g^{-1}) to this initial volume V_i, is calculated to be 0.722. It is interesting that p_i is by 3.1% lower than that estimated on the basis of slightly (within 30K) extrapolated $V-T$ results for OTP crystal phase $p_{cr}(T_i) = 0.745$, and further, that p_i lies in the vicinity of the limiting packing fraction for the closest ordered packing of hard spheres $p_{crhs} = 0.741$.[43] We note that the limiting packing fraction for the closest random packing of hard spheres is essentially lower 0.649.[43] This agreement between $T_{i,1}$ from a combination of dilatometric and PALS data ones via our model and T_K from calorimetry is quite acceptable. This is remarkable because both the results follow from the extrapolation of quite different quantities: the volume with free volume holes and the entropy. It can be considered as an argument in favor of the underlying phase transition taking place below T_g and of associated "ideal glass" concept which is, of course, experimentally inaccessible because of the well-known kinetic effects.[21-23]

In the literature, an approximate agreement between the Kauzmann temperature T_K and the Vogel temperature T_0 within 15−25 K has often been reported.[19b,22,23] It implies that $T_{i,1}$ might be related to T_0 as reported by us very recently.[44] In this connection we would like to stress that the Vogel eq 3 is not able to account for the *entire* viscosity or relaxation time range of ∼14 decades of magnitude.[1] In general, the T_0 value is a quite sensitive to the range of temperature interval ΔT used for a fitting with eq 3.[45] For this reason, a usual practice is to divide it into two separate temperature regions.[15] In the case of OTP this can be seen from our data compilation in Table 1. The first region from $T_g = 243$K up to about 290 ± 20K gives T_0 lying between 185 and 210 K. On the other hand, fitting the higher temperature data above 300 K provides $T_0 \cong T_g$. Keeping in mind these uncertainty, $T_{i,1}$ falls into the range of the T_0 values for the lower temperature data between T_g and 290 ± 20 K that is the interval of temperature used for the deducing the $T_{i,1}$ value. Despite approximate agreement between $T_{i,1}$ and T_0, we want to recall the above-mentioned robustness of solution of eq 15 with respect to choice of the input temperature. It suggests

TABLE 1: the Characteristic Temperatures of OTP: T_K (Kauzmann temperature) and T_0 (Vogel temperature) as Determined from Various Thermodynamic or Dynamic Properties, Respectively

process/method	temperature range, K	characteristic temperature T_{char}, K	ref
entropy/ calorimetry		T_K	
		200 ± 10	*a*
		200	*b*
		206.5	*c*
		205 ± 6	*d*
		204.2	*e*
primary α dynamics/ viscosity		T_0	
	243−293	200	*f*
	257−523	231	*f*
	300−416	248	*g*
	305−416	248	*h*
	243.5−343.5	199.4 ± 6.0	*i*
	240−320	192	*j*
	239−267	184	*k*
	270−416	246	*k*
	239−281	182	*l*
	281−551	250	*l*
	239−553	206	*l*
	240−251	170	*m*
dielectric spectroscopy	257−280	187	*l*
	246−268	202.4	*e*
photon correlation spectroscopy	258−285	209.4	*n*
	243−270	194	*o*
	243−270	185	*p*
specific heat spectroscopy		184 ± 13	*q*

[a] Greet, R. J.; Turnbull, D. *J. Chem. Phys.* **1967**, *47*, 2185. Hodge, L. M. *J. Non-Cryst. Solids* **1994**, *169*, 211. [b] Chang, S. S.; Bestul, A. B. *J. Chem. Phys.* **1972**, *56*, 503. Privalko, V. *J. Phys. Chem.* **1980**, *84*, 3307. [c] Murthy, S. S.; Paikaray, A.; Arya, N. *J. Chem. Phys.* **1995**, *102*, 8213. [d] Yamamuro, O.; Tsukushi, I.; Lindquist, A.; Takahara, S.; Ishikawa, M.; Matsuo, T. *J. Phys. Chem. B* **1998**, *102*, 1605 and private communication. [e] Richert, R.; Angell, C. A. *J. Chem. Phys.* **1998**, *108*, 9016. [f] Greet, R.; Turnbull, D. *J. Chem. Phys.* **1967**, *46*, 1243. [g] Laughlin, W. T.; Uhlmann, D. R. *J. Phys. Chem.* **1972**, *76*, 2317. [h] Cukierman, M.; Lane, J. W.; Uhlmann, D. R. *J. Chem. Phys.* **1973**, *59*, 3639. [i] Gerharz, B.; Meier, G.; Fischer, E. W. *J. Chem. Phys* **1990**, *92*, 7110. [j] Fischer, E. W. *Physica* **1993**, *A201*, 183. [k] Cummins H. Z. *Phys. Rev.* **1996**, *E54*, 5870. [l] Naoki, M.; Endou, H.; Matsumoto, K. *J. Phys. Chem.* **1987**, *91*, 4169. [m] Plazek, D.; Bero, C. A.; Chay, I. C. *J. Non-Cryst. Solids* **1994**, *172−174*, 181. [n] Fytas, G.; Wang, C. H.; Lilge, D.; Dorfmüller, *J. Chem. Phys.* **1981**, *75*, 4247. [o] Fischer, E. W.; Becker, Ch.; Hagenah, J. U.; Meier, G. *Prog. Colloid. Polym. Sci.* **1989**, *80*, 198. [p] Steffen, W.; Patkowski, A.; Meier, G.; Fischer, E. W. *J. Chem. Phys.* **1992**, *96*, 4171. [q] Dixon, P.; Nagel, S. R. *Phys. Rev. Lett.* **1988**, *61*, 341.

TABLE 2: Volumetric, Empty, and Hole-Free Volume Characteristic of OTP at the Two Important Temperatures T_g and T_r

quantity/unit	$T_g = 243$ K	$T_r = 304$ K
V, cm^3/g	0.8922	0.9320
$V_{f,e}$, cm^3/g	0.2654	0.3052
f_e	0.298	0.328
τ_3, ns	1.52	2.51
V_h, Å^3	56	149
$V_h/V^w \times 100$, %[a]	23.4	62.2
$V_{f,h}$, cm^3/g	0.0236	0.0672
I_3	0.40	0.41
f_h	0.027	0.073
c_hV, holes/cm^3 [b]	4.82×10^{20}	4.90×10^{20}
l_h, Å[c]	12.8	12.7

[a] Ratio of the mean hole volume V_h to the van der Waals volume V^w of OTP molecule; the latter being $V^w = 239.4$ Å^3 using an additive group scheme from ref 41. [b] The mean volume concentration of free volume holes. [c] The mean distance betweeen the mean free volume holes under assumption of their homogeneous distribution in the matrix.

the preference of $T_{i,1} \cong T_K$ identification over $T_{i,1} \approx T_0$ one. These findings may be considered as a support for the validity of one of the basic assumption of the original free volume model,[14,16,18] i.e., a linearity between f and T, eqs) or 7, respectively, but with $T_i \cong T_K$ instead of T_0. In other words, eq 10 implies that the free volume as measured by o-Ps probe and as treated by the present model seems to be simply an expansion volume of the supercooled liquid with respect to the initial volume V_i at T_i, where this excess dynamical free volume begins to appear due to some released degree of freedom, Figure 1.

Correlation between the Free Volume Hole Fraction and Viscosity. Calculating $V_g(T_g)$ from the V$-T$ data[27] and having both T_i and V_i from our model, we can calculate the free volume hole fraction $f_h(T)$ at the glass transition temperature T_g from eqs 10 and 11, then $f_h(T_g) = f_{h,g}$ is 2.7%. This value can be related to the so-called empty free volume $V_{f,e}$ at temperature T defined as[41]

$$V_{f,e}(T) = V(T) - V^w \qquad (25)$$

which represents the maximal geometric free volume of the matrix. From Table 2 it follows that the dynamic free volume hole fraction at T_g represents about 9% of the total empty space. The knowledge of $f_{h,g}$ opens up the possibility to determine the calibration coefficient $K_{V,h}$ in eq 2; $K_{V,h} = 1.2 \times 10^{-3}$ Å^{-3} and, consequently, to calculate the free volume hole fractions $f_h(T)$ at any temperature T from the PALS data *directly*.

Thus, we can test a possible relation between some representative dynamic quantity, e.g., viscosity and the measurable free volume hole fraction f_h from PALS method via the WLF$-$Doolittle-type equation by combining eqs 4 and 5. To make such a test we have to eliminate one of the three parameters by considering the ratio

$$\ln [\eta(T)/\eta(T_g)] = B_\eta[1/f_h(T) - 1/f_h(T_g)] \qquad (26)$$

as usually made in the WLF approach.[1c,14] If the viscosity$\eta$is governed by the free volume hole fraction from PAL:S, then the particular B_η coefficient is expected to be constant in the temperature range of the validity of eq 26. The result of such a test on the viscosity data of OTP from ref 46, which are considered to be the most precise ones, is shown in Figure 4. These data, as obtained by several authors over a wide T range, have been accounted for by two VFTH eqs; one for the low T region and the other for higher temperatures with intersection point at 283.3 K. We can found a quite satisfactory fit over

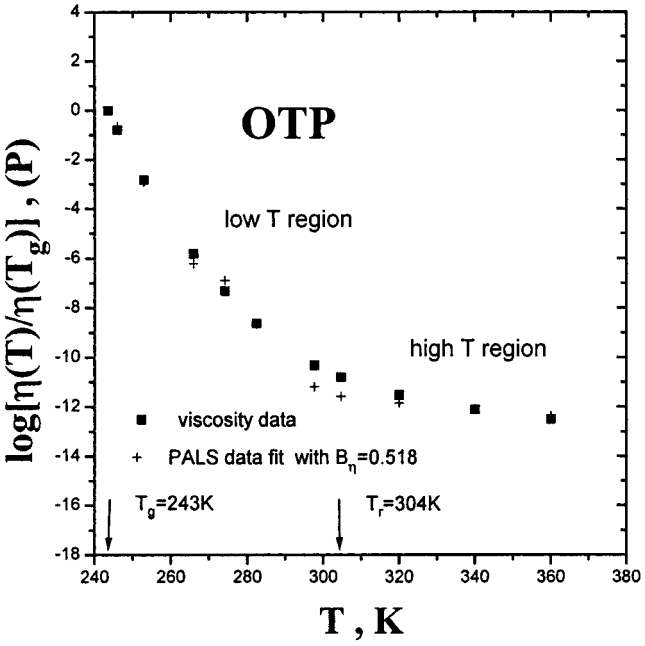

Figure 4. Correlation between the viscosity data of OTP from ref 46 and the free volume hole fraction f_h as determined from the PALS data (ref 28) by means of the presented model in terms of the WLF$-$Doolittle type equation.

12.5 decades of the change of viscosity between $T_g = 243$ and 360 K with $B_\eta = 0.518$. Note that although the T_i and V_i data and consequently, K_{Vh} coefficient have been determined from the low T region PALS data only, the free volume hole fractions for the high T range have been calculated with the same coefficient. This correlation indicates that the free volume hole fraction $f_h(T)$ as measured by means of PALS method of the relevance to the viscosity over the whole temperature interval measured by both the methods so far.

Crossover Liquid$-$Liquid Transition and Fluid Liquid Region. The specific volume vs temperature plot for amorphous OTP in ref 27 shows the monotonic course from T_g up to T_m and beyond. On the other hand, the τ_3-T plot in ref 28 exhibits the relatively strong increase in the range between T_g and $T_r = 304$ K followed by relatively mild growth above T_r. This "decoupling" effect of the total volume and of the free volume holes above the characteristic temperature T_r seems to be indication of the change of o-Ps$-$matrix interaction mechanism as believed already in the original paper.[27] The results of our more realistic calculations using the modified bubble model in section IIIB plotted in Figure 2 can be discussed as follows.

In the low-temperature region from T_g up to T_r, the predicted bubble sizes exceed the mean free volume hole sizes from the PALS data as evaluated by eq 1. Simultaneously, the expansivity of bubble and that of free volume holes given by the corresponding slopes in eqs 24 and 19b differ essentially; the former being 1 order of magnitude lower than the latter. It indicates that at temperatures below T_r, the o-Ps probes indeed feel the original preexisting holes and that the matrix has relatively rigid character. As for the higher temperature region, the predicted bubble sizes exceed the mean free volume hole over 26%, although the corresponding expansivities are similar. Evidently, the first finding means that the modified bubble concept does not work for the fluid liquid state of OTP. Moreover, the above-mentioned correlation between the free volume hole fraction and viscosity (Sect.IVB) holds for both the low and high T regions. Thus, we conclude that the bubbles can be excluded in the high-temperature region of OTP.

Relationship of the Free Volume Microstructure to Other Dynamic Phenomena. Table 2 contains some free volume hole characteristics of OTP at two important temperatures T_g and T_r. They give us more insight into the free volume situation in this important glass-former and can be used in interpretations of further dynamic properties.

For example, from Figure 2 and Table 2, it is evident that the free volume holes are essentially smaller than the van der Waals volume of OTP molecule. It implies that any dynamic process must be highly cooperative in agreement with the high fragility of OTP.[23] According to the so far qualitative explanation,[23] high fragility, i.e., the strong change of viscosity with temperature, is attributed to the large structural reorganization during the temperature change above T_g. Further, although the free volume hole fraction increases from 2.7% at T_g to 7.3% at T_r, the mean free volume hole concentration grows more slightly due to the fact that the main contribution comes from the increase of mean free volume hole size rather than from the increase of their population. The pronounced free volume hole size expansion coefficient above T_g, $\alpha_{Vh} = 2.56 \times 10^{-2}$ K^{-1}, may be related to the thermal expansion of the mean square displacements of hydrogen atoms from neutron scattering study[47] $\alpha_{\langle u^2 \rangle} = 2.1 \times 10^{-2}$ K^{-1}. Recently, we have found the same relationships for a series of polymers.[8,9] These findings suggest a common origin of both the phenomena, i.e., the dynamic free volume hole expansion and the expansion of the geometric characteristic of the microscopic mobility.

In the original PALS work,[28] a suggestion has been made concerning the possible connection between T_r and the so-called crossover (or critical) temperature T_c from preliminary application of the mode coupling (MCT)[1d] on OTP. Since the time of publication, numerous experimental tests of the ideal version MCT predictions for OTP have been performed.[46−51] On the basis of the successful fitting the high-temperature viscosity data by the power law equation[1d] as well as of the anomaly behavior of the Debye−Waller factor T_c was estimated to be 290 ± 5 K.[48,51] According to MCT, at this temperature purely dynamic transition takes place which is characterized by a critical slowing down of the density fluctuations. In addition, there are further important experimental findings such as the results of the corresponding state analysis applied to viscosity and rotational correlation times,[50] a bifurcation of single liquid relaxation process at high temperatures into the primary α relaxation and the slow secondary β_s one[52] as well as the breakdown of the Stokes−Einstein relation for the translational diffusion $D_{tr} \sim 1/\eta$ below T_c.[52,53] All these findings indicate the crossover between two distinct dynamic regimes at the critical temperature $T_c \cong (1.18-1.28)T_g$.[52,53] These dynamic facts are fully consistent with the appearance of the characteristic temperature T_r in PALS measurement as well as with our physical picture of supercooled liquid as relatively little defective quasi-rigid viscous liquid below $T_r \sim T_c$ and very defective and soft fluid liquid phase above T_r.

V. Summary

A phenomenological model linking the macroscopic volume to the microscopic free volume has been formulated in order to quantify the free volume hole fraction by determining the proportionality coefficient K_{Vh}. The most important output is the finding of the so-called initial temperature T_i, at which dynamic free volume begins to appear. Its application on a typical fragile low molecular weight glass former, *o*-terphenyl, leads to the T_i value which is in acceptable agreement with the Kauzmann temperature T_K. These findings seem to support the original, free volume model of transport properties in disordered media[14,16,19] by (i) confirming the assumption of linearity between the free volume and temperature in the viscous region and (ii) identification of the free hole volume as the excess volume over the initial liquid one V_i at T_i. For the first time, the viscosity data on OTP over more than 12 decades of the change of magnitude have been directly correlated with the free volume hole fractions from the PALS data via the present model.

Acknowledgment. We would like to thank the VEGA Agency for support this work by Grants 2/4008/97 and 2/5080/98.

References and Notes

(1) (a) Richert, R.; Blumen, A. Eds. *Disordered Effects on Relaxational Processes*; Springer-Verlag: Berlin, 1994. (b) Rössler, E.; Sillescu, H. In *Material Science and Technology*; Yaryzcki, J., Ed.; Chemie Verlag: Weinheim, 1991; Vol. 9 (Glasses and Amorphous Materials), p 573. (c) Ferry, J. D. *Viscoelastic Properties of Polymers*; Wiley: New York, 1980. (d) Götze, W.; Sjörgen, L. *Rep. Prog. Phys.* **1992**, *55*, 241. (e) Ediger, M. D.; Angell, C. A.; Nagel, S. R. *J. Phys. Chem.* **1996**, *100*, 13200. (f) Cummins, H. Z.; Li, G.; Hwang, Y. H.; Shen, G. O.; Du, W. M.; Hernandez, J.; Tao, N. J. *Z. Phys. B* **1997**, *103*, 501.

(2) Kovacs, A. J. *Fortschr. Hochpolym.−Forsch.* **1963**, *3*, 394.

(3) Jean, Y. C. *Microchem. J.* **1990**, *42*, 72.

(4) Jean, Y. C. in *Positron Spectroscopy of Solids*; Dupasquier, A., Mills, A. P., Jr., Eds.; IOS, Ohmsha: Amsterdam, 1995; p 563.

(5) Brand, W.; Dupasquier, A. *Positron Solid State Physics*; Schrader, D. M., Jean, Y. C., Eds.; Elsevier: Amsterdam, 1988.

(6) Nakanishi, H.; Jean, Y. C. In *Positron and Positrinium Chemistry*; Schrader, D. M., Jean, Y. C., Eds.; Elsevier: Amsterdam, 1988.

(7) Kluin, J.; Yu, Z.; Vleeshouvers, S.; McGervey, J. D.; Jamieson, A. M.; Simha, R. *Macromolecules* **1992**, *25*, 5089.

(8) Bartoš, J.; Krištiak, J.; T. Kanaya, T. *Physica* **1997**, *B234−236*, 435.

(9) Bartoš, J.; Bandžuch, P.; Šauša, O.; Krištiaková, K.; Krištiak, J.; Jenninger, W. *Macromolecules* **1997**, *30*, 6906.

(10) Kobayashi, Y.; W. Zheng, W.; Meyer, E. F.; McGervey, J. D.; Jamieson, A. M.; Simha, R. *Macromolecules* **1989**, *22*, 2302.

(11) Wang, Y. Y.; Nakanishi, H.; Jean, Y. C.; Sandreczki, T. C. *J. Polym. Sci. B Polym. Phys.* **1990**, *28*, 1431.

(12) Hristov, H. A.; Bolan, B.; Yee, A. F.; Xie, L.; Gindley, D. W. *Macromolecules* **1996**, *29*, 8507.

(13) (a) Vogel, H. *Phys. Z.* 1921, *22*, 645. (b) Fulcher, G. S. *J. Am. Ceram. Soc.* **1925**, *8*, 339. (c) Tammann, G.; Hesse, W. *Allg. Chem.* **1926**, *156*, 245.

(14) Williams, M. L.; Landel, R. F.; Ferry, J. D. *J. Am. Chem. Soc.* **1955**, *77*, 3701.

(15) (a) Barlow, A. J.; Lamb, J.; Matheson, A. J. *Proc. R. Soc.* **1966**, *A292*, 322. (b) Stickel, F.; Fischer, E. W.; Richert, R. *J. Chem. Phys.* **1996**, *104*, 2043.

(16) Fox, T.; Flory, P. J. *J. Appl. Phys.* **1950**, *21*, 581.

(17) Doolittle, A. K. *J. Appl. Phys.* **1951**, *22*, 1471.

(18) (a) Cohen, M. H.; Turnbull, D. *J. Chem. Phys.* **1959**, *31*, 1164. (b) Turnbull, D.; Cohen, M. H. *J. Chem. Phys.* **1961**, *34*, 120. (c) Turnbull, D.; Cohen, M. H. *J. Chem. Phys.* **1970**, *52*, 3038.

(19) (a) Cohen, M. H.; Grest, G. S. *Phys. Rev.* **1979**, *B20*, 1077. (b) Grest, G. S.; Cohen, M. H. *Adv. Chem. Phys.* **1981**, *48*, 455.

(20) (a) Gibbs, J. H.; DiMarzio, E. A. *J. Chem. Phys.* **1958**, *28*, 373. (b) Adam, Gibbs, J. H. *J. Chem. Phys.* **1965**, *43*, 139.

(21) Kauzmann, W. *Chem. Rev.* **1948**, *43*, 219.

(22) Hodge, I. M. *J. Non-Cryst. Solids* **1994**, *169*, 211.

(23) Angell, C. A. *J. Res. Nat. Inst. Stand.* **1997**, *102*, 171.

(24) (a) Cohen, M. H.; Turnbull, D. *Nature* **1964**, *203*, 9645. (b) Nelson, D. R. *Phys. Rev. Lett.* **1983**, *50*, 982. (e) Sethna, J. P. *Europhys. Lett.* **1988**, *6*, 529. (f) Kirkpatrick, T. R.; Thirumalai, D.; Wolynes, P. G. *Phys. Rev.* **1989**, *A40*, 1045. (g) Sachdev, S. In *Bond Orientational Order in Condensed Matter Systems*; Standburg, K. J., Ed.; Springer- Verlag: New York, 1992.

(25) Anderws, J. N.; Ubbelohde, A. R. *Proc. R. Soc.* (*London*) **1955**, *A228*, 435.

(26) Greet, R. J.; Turnbull, D. *J. Chem. Phys.* **1967**, *46*, 1243.

(27) Naoki, M.; Koeda, S. *J. Phys. Chem.* **1989**, *93*, 948.

(28) Malhothra, B. D.; Pethrick, R. A. *J. Chem. Soc., Faraday Trans. 2* **1982**, *78*, 297.

(29) Malhotra, B. D.; Pethrick, R. A. *Phys. Rev.* **1983**, *B28*, 1256.

(30) Ferrell, R. A. *Phys. Rev.* **1957**, *108*, 167.

(31) Roelling, L. O.; Kelly T. M. *Phys. Rev. Lett.* **1967**, *18*, 387.

(32) Tao, S. J. *J. Chem. Phys.* **1972**, *56*, 5499.

(33) Mogensen, O. E. *Electrochim. Acta* **1988**, *33*, 1203.

(34) Gregory, R. B.; Chai, K. J. *Mater. Sci. Forum* **1992**, *105−110*, 1573.
(35) Byakov, V. M. Private communication.
(36) Tolman, R. C. *J. Chem. Phys.* **1947**, *17*, 2185.
(37) Grest, R. J.; Turnbull, D. *J. Chem. Phys.* **1967**, *47*, 2185.
(38) Privalko, V. *J. Phys. Chem.* **1980**, *84*, 3307.
(39) Murthy, S. S.; Paikaray, A.; Arya, N. *J. Chem. Phys.* **1995**, *102*, 9213.
(40) Richert, R.; Angell, C. A. *J. Chem. Phys.* **1998**, *108*, 9016.
(41) Bondi, A. *Physical Properties of Molecular Crystals, Liquids and Glasses*; Wiley: New York, 1968.
(42) Askadskii, A. A. *Usp. Chim.* **1977**, *46*, 1122.
(43) Jordrey, W. S.; Tory, E. M. *Phys. Rev.* **1985**, *A32*, 2341.
(44) Krištiak, J.; Bartoš, J.; Šauša, O.; Bandžuch, P. *Mater. Sci. Forum* **1997**, *255−257*, 35.
(45) Dixon, P. K. *Phys. Rev.* **1990**, *B42*, 8179.
(46) Cicerone, M. T.; Ediger, M. D. *J. Phys. Chem.* **1993**, *97*, 10 489.
(47) (a) Bartsch, E.; Fujara, F.; Kiebel, M.; Sillescu, H.; Petry, W. *Ber. Bunsen-Ges. Phys. Chem.* **1989**, *93*, 1525. (b) Petry, W.; Batrsch, E.; Fujara, F.; Kiebel, M.; Sillescu, H.; Farago, B. *Z. Phys.* **1991**, *B83*, 175.
(48) Fujara, F. *J. Mol. Struct.* **1993**, *296*, 285.
(49) Bartsch, E.; Fujara, F.; Geil, B.; Kiebel, M.; Petry, E.; Schnauss, W.; Sillescu, H.; Wuttke, J. *Physica* **1993**, *A201*, 223.
(50) Rössler, E. *Ber. Bunsen-Ges. Phys. Chem.* **1990**, *94*, 392.
(51) Cummins, H. Z.; Li, G.; Du, W.; Hwang, Y. H.; Shen, G. O. *Prog. Theor. Phys., Suppl.* **1997**, *126*, 21.
(52) Rössler, E. *Phys. Rev. Lett.* **1990**, *65*, 1595.
(53) (a) Fujara, F.; Geil, B.; Sillescu, H.; Fleischer, G. *Z. Phys. B: Condens. Matter* **1992**, *88*, 195. (b) Chang, I.; Fujara, F.; Geil, B.; Heuberger, G.; Mangel, T.; Sillescu, H. *J. Non-Cryst. Solids* **1994**, *172−174*, 248.